Biophysical Chemistry 156 (2011) 3–12

Contents lists available at ScienceDirect

Biophysical Chemistry

journal homepage: http://www.elsevier.com/locate/biophyschem

Review

Volumetric measurements in binary solvents: Theory to experiment

Tigran V. Chalikian *

Department of Pharmaceutical Sciences, Leslie Dan Faculty of Pharmacy, University of Toronto, 144 College Street, Toronto, Ontario M5S 3M2, Canada

ARTICLE INFO

Article history:
Received 10 November 2010
Received in revised form 10 December 2010
Accepted 11 December 2010
Available online 24 December 2010

Keywords:
Cosolvents
Proteins
Thermodynamics
Volume
Compressibility

ABSTRACT

Interactions of proteins and protein groups with water-soluble cosolvents have been studied for the last 50 years with a variety of theoretical and experimental methods. The contribution of volumetric techniques to these studies is relatively modest, although volumetric properties of solutes are sensitive to the entire spectrum of solute–solvent and solute–cosolvent interactions. This deficiency is partly related to formidable experimental difficulties related to conducting volumetric measurements at high cosolvent concentrations and partly to the lack of the theoretical framework within which volumetric results can be rationalized in terms of solute–solvent and solute–cosolvent interactions. However, recent years have witnessed a revival of interest in application of the volumetric approach to characterization of solute–solvent interactions in protein solutions in binary mixtures. This review presents an overview of recent advances in the field, focusing on both the theoretical and the experimental developments. While presenting the current state of the art, it also outlines the strategy for future volumetric studies that will result in new insights into the old problem of interactions of proteins with protecting and denaturing osmolytes.

Contents

1. Introduction

Interactions of a protein with the components of the surrounding solvent represent a major force determining and guiding processes of folding and binding [1–3]. The solvent is invariably water to which more or less significant amounts of water-miscible compounds may be added. Binary solvents, representing a concentrated mixture of a cosolvent and water as the principal solvent, are of special interest from both the biological and the physico-chemical viewpoints [4–6]. The added cosolvent may exert a stabilizing or destabilizing influence on the native conformation of a protein or may be neutral. Organic cosolvents are often referred to as osmolytes, since they are used by cells of a variety of organisms to counteract the osmotic loss of cell water.

Attempts to understand and describe the differential thermodynamics of solute–solvent versus solute–cosolvent interactions have attracted considerable effort from both experimental and theoretical research groups [7–10]. These efforts have begun to provide us with the structural and thermodynamic details needed for elucidating the molecular origins of the stabilizing/destabilizing action of various osmolytes.

* Tel.: +1 416 946 3715; fax: +1 416 978 8511.
E-mail address: chalikan@phm.utoronto.ca.

0301-4622/$ – see front matter © 2010 Elsevier B.V. All rights reserved.
doi:10.1016/j.bpc.2010.12.004

A rigorous thermodynamic way of characterizing the mode of action of a specific cosolvent on a protein is in terms of preferential interaction parameter, $(\partial\mu_3/\partial m_2)_{m3} = (\partial\mu_2/\partial m_3)_{m2}$, or preferential binding parameter $\Gamma_{23} = (\partial m_3/\partial m_2)_{\mu3} = -[(\partial\mu_3/\partial m_2)_{m3}/(\partial\mu_3/\partial m_3)_{m2}] = -(\partial\mu_2/\partial\mu_3)_{m2}$, where μ_i and m_i are, respectively, the chemical potential and molal concentration of component *i* [1,11,12]. Here and further below, we use a notation in which components 1, 2, and 3 correspond to water, solute under investigation, and cosolvent, respectively. Another way of describing solute–cosolvent versus solute–water interactions is based on measuring the free energy of the transfer of a solute from water to a cosolvent solution, $\Delta\mu_{tr}$. Transfer free energy is related to preferential interaction parameter through $\Delta\mu_{tr} = \int_0^{m3} (\partial\mu_2/\partial m_3)_{m2} dm_3$.

The Kirkwood–Buff theory has been applied to investigating solvation of a solute in binary solvents consisting of water and cosolvent [9,10,13–23]. This is an exact statistical mechanical theory that links the radial distribution functions, $g_{ij}(r)$, between the different solution components with their thermodynamic properties including partial molar volumes and compressibilities [24–27]. These properties are expressed *via* the Kirkwood–Buff integrals $G_{ij} = 4\pi\int_0^\infty \left[g_{ij}(r)-1\right] r^2 dr$ which can be readily calculated if the radial distribution functions $g_{ij}(r)$ are known. The Kirkwood–Buff integral can be expressed as $G_{ij} = -V_{ij} + I_{ij}$, where V_{ij} represents the effect of excluded volume of the solute with respect to the solvent or cosolvent, while I_{ij} is the interaction term that describes the volume effect of solute–solvent and solute–cosolvent interactions [29]. If a specific solvent component is preferentially bound to the solute, its density around the solute is higher than that in the bulk with the resulting positive contribution to the I_{ij} term. In contrast, if a cosolvent is preferentially excluded from the solvation shell of a solute, the cosolvent contribution to I_{ij} is negative. These simple considerations provide the basis of applications of Kirkwood–Buff integrals to quantifying the concepts of preferential binding and exclusion.

These theoretical considerations parallel the analysis presented by Schellman [5,29] and Davis-Searle et al. [30]. Based on the combination of the solvent exchange model with scaled particle theory, it has been proposed that the water-to-osmolyte transfer free energy may be divided into two components. One component is represented by the unfavorable free energy of cavity formation (excluded volume effect) that is opposed by a generally favorable change in free energy associated with the formation of solute–cosolvent interactions. The net change in free energy accompanying the water-to-osmolyte transfer and, consequently, the mode of action of a specific osmolyte depend on the balance between these contributions.

It is within these lines that volumetric measurements have proven useful in providing unique characterization of the differential thermodynamics of solute–cosolvent versus solute–water interactions. Volumetric parameters of a solute are influenced by both the cavity, that should be created in the solvent to accommodate the solute, and the manifold of solute–solvent interactions. Volumetric observables, including the partial molar volume, compressibility, and expansibility of a solute, have been widely employed for characterizing its hydration (solute–solvent interactions in pure water) [31–42]. However, until recently, volumetric measurements have been applied rarely to investigations of solvation in binary solvents. This deficiency is related to experimentally demanding measurement protocols due to the high cosolvent concentration and to the lack of a conceptual formalism that can be used for microscopic interpretation of measured macroscopic data. In this work, we review recent progress in the use of volumetric measurements in studying solvation in binary solvents and present theoretical links between macroscopic volumetric data and microscopic properties of the ternary system consisting of a solute, cosolvent, and water.

2. Solvation models and links to thermodynamics

Interpretation of volumetric data is generally performed within the framework of models in which solvent in the bulk domain is compositionally and thermodynamically distinct from the solvent in the vicinity of the solute [2,11,12]. In these models, solute–solvent and solute–cosolvent interactions perturb the local concentrations of solvent components in the regions adjacent to the solute thereby leading to preferential binding (a local increase in cosolvent concentration over the concentration in the bulk) or preferential hydration (a local increase in water concentration). Solute-perturbed solvent does not form any rigid shell of strongly bound water and cosolvent molecules around the solute, although some more or less tightly bound water and cosolvent molecules may be present in the solvation shell. Instead, the solvation shell represents a fluctuating cloud of perturbed water and cosolvent molecules that interact either favorably or unfavorably with solvent-exposed groups of a solute [2]. The surface of a solute can be presented as consisting of loci that can interact with water and cosolvent with varying affinity. Each locus may have a stronger affinity for water, for solvent, or be indifferent. These varying affinities and their spatial arrangements dictate the formation of the local structure, dynamics, and composition of the solvation shell which are formed in a manner that depends on cosolvent concentration. As a conceptual practicality, the solvation layer of a solute can be described as comprising of n_1 perturbed water molecules and n_3 perturbed cosolvent molecules. Importantly, the operationally defined numbers n_1 and n_3 do not correspond only to the solvent molecules in direct contact with a solute but, more generally, refer to all water and cosolvent molecules which are thermodynamically perturbed by the solute.

In a number of studies, expressions that connect the preferential binding, Γ_{23}, and preferential hydration, Γ_{21}, parameters with the effective numbers of cosolvent, n_3, and water, n_1, molecules interacting with the solute have been derived [2,11,12,43]. The preferential binding parameter, Γ_{23}, is related to n_3 and n_1 *via* $\Gamma_{23} = n_3 - (m_3/m_1)n_1$ [1,11,44,45]. Similarly, the preferential hydration parameter, $\Gamma_{21} = (\partial m_1/\partial m_2)_{\mu1}$, is given by $\Gamma_{21} = n_1 - (m_1/m_3)n_3$. It should be noted that, while the preferential binding, Γ_{23}, and hydration, Γ_{21}, parameters are rigorous, experimentally measurable thermodynamic parameters, n_1 and n_3 are not. Firstly, n_1 and n_3 are interrelated. Secondly, n_1 and n_3 are vaguely defined as, respectively, the numbers of water and cosolvent molecules within some volume around the solute. This volume should be reasonably large to comprise all solute-perturbed water and cosolvent molecules. Given this vague definition, it is clear that there is no unique pair of n_1 and n_3 values that satisfies the above given equations for Γ_{23} and Γ_{21}.

Solvent perturbation by the solute results in changes in virtually every thermodynamic parameter of the solvent components including their standard chemical potential, μ°, and the volumetric properties partial molar volume, V°, adiabatic, K°_S, and isothermal, K°_T, compressibility, and expansibility, E°. Consequently, volumetric measurements, if properly designed and interpreted, may provide valuable new insights into the solvation properties of solutes in binary solvents including solute–water and solute–cosolvent interactions.

3. Volumetric observables and microscopic interpretation

3.1. Simplistic continuous model

In this empirical model, the partial molar volume, V°, of a solute at any particular cosolvent concentration can be presented as follows:

$$V^\circ = V_C + n_1(V_{1h} - V_{10}) + n_3(V_{3h} - V_{30}) + \beta_{T0}RT \quad (1)$$

where $V_C = V_M + V_T$ is the volume of the cavity in the solvent enclosing a solute; V_M is the intrinsic volume of a solute which

represents its geometric volume inaccessible to solvent molecules; the term V_T is collectively referred to as thermal volume and represents the "void" volume around the solute due to the steric, vibrational, and structural effects; V_{1h} and V_{10} are the partial molar volumes of water in the solvation shell of a solute and in the bulk, respectively; V_{3h} and V_{30} are the partial molar volumes of the cosolvent in the solvation shell of a solute and in the bulk, respectively; and β_{T0} is the coefficient of isothermal compressibility of the solvent.

The steric component of V_T reflects the imperfect packing of solute and solvent molecules in the solution. The vibrational component results from thermally-induced mutual vibrational motions of solute and solvent molecules and, theoretically, should subside to zero at 0 K. The structural component reflects the open (tetrahedral) structure of water and related packing effects around solute molecules.

The respective relationships for the partial molar isothermal compressibility, $K_T^\circ = -(\partial V^\circ/\partial P)_T$, and expansibility, $E^\circ = (\partial V^\circ/\partial T)_P$, of a solute are the following:

$$K_T^\circ = K_C + n_1(K_{1h}-K_{10}) + n_3(K_{3h}-K_{30}) - (\partial n_1/\partial P)_T(V_{1h}-V_{10}) - (\partial n_3/\partial P)_T(V_{3h}-V_{30}) - (\partial \beta_{T0}/\partial P)_T RT \quad (2)$$

$$E^\circ = E_C + n_1(E_{1h}-E_{10}) + n_3(E_{3h}-E_{30}) + (\partial n_1/\partial T)_P(V_{1h}-V_{10}) + (\partial n_3/\partial T)_P(V_{3h}-V_{30}) + R[\beta_{T0} + T(\partial \beta_{T0}/\partial T)_P] \quad (3)$$

where K_{1h} and K_{10} are the partial molar isothermal compressibilities of water in the solvation shell of a solute and in the bulk, respectively; E_{1h} and E_{10} are the partial molar expansibilities of water in the solvation shell of a solute and in the bulk, respectively; K_{3h} and K_{30} are the partial molar isothermal compressibilities of the cosolvent in the solvation shell of a solute and in the bulk, respectively; E_{3h} and E_{30} are the partial molar expansibilities of the cosolvent in the solvation shell of a solute and in the bulk, respectively.

The model and Eq. (1) can be used in simple qualitative analyses of the partial molar volume of a solute. The additivity inherent to Eq. (1) cannot be generally extended to the partial molar isothermal, K°_T, or adiabatic, K°_S, compressibility and expansibility, E°, of a solute due to non-zero values of the derivatives $(\partial n_1/\partial P)_T$, $(n_3/\partial P)_T$, $(\partial n_1/\partial T)_P$, and $(\partial n_3/\partial T)_P$. These derivatives do not generally correlate to the effective numbers of water, n_1, and cosolvent, n_3, within the solvation shell of a solute and cannot be evaluated without application of additional models/assumptions on solute–solvent interactions.

3.2. Kirkwood–Buff theory

As noted above, the Kirkwood–Buff theory is an exact statistical mechanical theory that links the radial distribution functions, $g_{ij}(r)$, between the different solution components with their thermodynamic properties including partial molar volumes and compressibilities [24–27]. These properties are expressed *via* the Kirkwood–Buff integrals $G_{ij} = \int_0^\infty [g_{ij}(r)-1]4\pi r^2 dr$. Significantly, the Kirkwood–Buff integrals can also be evaluated in an alternative (inversion) procedure from experimental data (density, compressibility, and activity coefficient derivatives) in the absence of the knowledge of specific radial distribution functions $g_{ij}(r)$ [28].

The preferential hydration parameter, Γ_{21}, is related to the Kirkwood–Buff integrals via the expression:

$$\Gamma_{21} = N_{21} - (C_1/C_3)N_{23} \quad (4a)$$

where C_1 and C_3 are the molarities of water and cosolvent, respectively; $N_{21} = N_A C_1 G_{21}$ and $N_{23} = N_A C_3 G_{23}$ are, respectively, the excess numbers of water and cosolvent in the region including the solute proper and its immediate surroundings; and N_A is Avogadro's number [9,46].

Similarly, the preferential binding parameter is given by the relationship:

$$\Gamma_{23} = -(C_3/C_1)\Gamma_1 = N_{23} - (C_3/C_1)N_{21}. \quad (4b)$$

In a number of publications from the Shimizu group, it has been suggested that preferential interaction measurements can be combined with partial molar volume measurements to evaluate the excess hydration, N_{21}, and solvation, N_{23}, numbers [9,10,19]. In fact, the Kirkwood–Buff theory gives an expression for the partial molar volume, V°, of a solute in terms of the Kirkwood–Buff integrals. For the limit of very dilute solution of the solute, its partial molar volume in the mixture of solvent and cosolvent is given by the expression [26,27]:

$$V^\circ = -C_1V_1G_{21} - C_3V_3G_{23} + \beta_{T0}RT = -N_{21}V_1 - N_{23}V_3 + \beta_{T0}RT. \quad (5)$$

Shimizu has proposed that the excess numbers of N_{21} and N_{23} can be calculated from experimental data by solving Eq. (4a) or (4b) and Eq. (5). On a similar note, changes in N_{21} and N_{23} associated with a biochemical reaction involving the solute can be calculated from the parallel measurements of changes in preferential hydration, $\Delta\Gamma_{21}$, or binding, $\Delta\Gamma_{23}$, parameter and a change in volume, ΔV, associated with the reaction:

$$\Delta\Gamma_{21} = \Delta N_{21} - (C_1/C_3)\Delta N_{23} \quad (6a)$$

$$\Delta\Gamma_{23} = \Delta N_{23} - (C_3/C_1)\Delta N_{21} \quad (6b)$$

$$\Delta V = -\Delta N_{21}V_1 - \Delta N_{23}V_3. \quad (7)$$

This approach in conjunction with experimental data on preferential interaction parameter and partial molar volume has been successfully implemented in analyzing solvation properties of proteins as well as changes in these properties accompanying protein denaturation and ligand–protein and protein–protein binding events [9,10,17,19]. In particular, the values of N_{21} and N_{23} or $G_{21} = N_{21}/(N_A C_1)$ and $G_{23} = N_{23}/(N_A C_3)$ have been evaluated for ribonuclease T1 in aqueous urea solutions and ribonuclease A in aqueous trehalose solutions [19]. The Kirkwood–Buff parameter, G_{23}, of ribonuclease A in water/trehalose mixtures has been found to be much smaller than the parameter G_{21} signifying preferential exclusion of trehalose from the protein surface. In contrast, the values of G_{23} and G_{21} of ribonuclease T1 in water/urea mixtures are very similar. This similarity coupled with the larger size of urea molecules relative to water has been interpreted as suggesting accumulation of urea in the vicinity of the protein [19].

3.3. Statistical thermodynamics-based solvent exchange model

Principles of statistical thermodynamics have been recently applied to derivation of the theoretical framework that can be used for interpretation of volumetric data [47,48]. In a system consisting of a solute dissolved in a binary mixture of the principal solvent (water) and the cosolvent (osmolyte), solute–solvent interactions can be considered within the framework of a set of chemical reactions, in which a solute associates with *i* water (W) and *j* osmolyte (O) molecules:

$$S_0 + iW + jO \leftrightarrow SW_iO_j \quad \text{(Reaction 1)}$$

where S_0 signifies a solute species that, while being in solution, does not interact with either water or the cosolvent.

Each reaction is characterized by a binding free energy, ΔG_{ij}, that is contributed by the formation of direct solute–solvent and solute–

cosolvent interactions and disruption of pre-existing solvent–solvent and solvent–cosolvent (and, possibly, cosolvent–cosolvent) interactions. Therefore, ΔG_{ij} may exhibit a range of values extending from negative (favorable interactions) to positive (unfavorable interactions). The net concentration of a solute in solution can be expressed *via* the binding polynomial:

$$[S_l] = \sum_j \sum_i \left[SW_iO_j\right] = [S_0] \sum_{j=0}^{n/r} \sum_{i=0}^{n-jr} a_1^i a_3^j \, exp\left(-\Delta G_{ij}/RT\right) \tag{8}$$

where a_1 and a_3 are the activities of the principal solvent and the cosolvent, respectively; n is the maximum number of solvent-binding sites of a solute; r is the number of solvent molecules displaced by a cosolvent molecule upon its association with the solute.

Solvation can be defined as a process in which a solute is transferred from a fixed position in the ideal gas phase to a fixed position in the liquid (solution) phase [26,27,49]. The Gibbs free energy of solvation, ΔG^*, is the reversible work required for such a transfer and equals the average binding energy (coupling work) of a solute with the solvent components at some fixed configuration:

$$\Delta G^* = -RT \, ln\left([S_l]/\left[S_g\right]\right) \tag{9}$$

where $[S_g]$ is the molar concentrations of a solute in the ideal gas phase that exists in equilibrium with the solute in the liquid phase [26,27,49].

Combining Eqs. (8) and (9), one obtains the expression for solvation Gibbs free energy:

$$\begin{aligned}\Delta G &= -RT \, ln\left([S_l]/\left[S_g\right]\right) = -RT \, ln\left([S_0]/\left[S_g\right]\right) \\ &\quad -RT \, ln\left[\sum_{j=0}^{n/r} \sum_{i=0}^{n-jr} a_1^i a_3^j \, exp\left(-\Delta G_{ij}/RT\right)\right] = G_C + G_I\end{aligned} \tag{10}$$

where $G_C = -RTln([S_0]/[S_g])$ is the free energy of solvation of the noninteracting solute species which corresponds to the free energy of formation of a cavity in the solvent that is sufficiently large to accommodate the solute; and $G_I = -RT \, ln\left[\sum_{j=0}^{n/r} \sum_{i=0}^{n-jr} a_1^i a_3^j \, exp(-\Delta G_{ij}/RT)\right]$ is the free energy of direct interactions of solute with the components of the solvent.

The partial molar volume, V°, of a solute is given by the relationship [47,48]:

$$\begin{aligned}V^\circ &= \left(\partial \Delta G^*/\partial P\right)_T + \beta_T RT = V_C + \sum_{j=0}^{n/r} \sum_{i=0}^{n-jr} \alpha_{ij} \Delta V_{ij} + \beta_T RT \\ &= V_C + <\Delta V> + \beta_T RT\end{aligned} \tag{11}$$

where $V_C = (\partial G_C/\partial P)_T$ is the volume of the cavity enclosing the solute; $\alpha_{ij} = a_1^i a_3^j \, exp(-\Delta G_{ij}/RT) \Big/ \left[\sum_{j=0}^{n/r} \sum_{i=0}^{n-jr} a_1^i a_3^j \, exp(-\Delta G_{ij}/RT)\right]$ is the fractional composition of the solute species SW_iO_j; $\Delta V_{ij} = (\partial \Delta G_{ij}/\partial P)_T$ is the volume effect of formation of the solvated complex with i water and j cosolvent molecules; and $<\Delta V> = \sum_{j=0}^{n/r} \sum_{i=0}^{n-jr} \alpha_{ij} \Delta V_{ij}$ is the ensemble average change in volume associated with direct solute–solvent interactions.

Differentiation of Eq. (11) with respect to pressure and temperature yields the relationship for partial molar isothermal compressibility, $K_T^\circ = -(\partial V^\circ/\partial P)_T$, and expansibility, $E^\circ = (\partial V^\circ/\partial T)_P$ [48]:

$$K_T^\circ = K_C + <\Delta K_T> + \left(<\Delta V^2> - <\Delta V>^2\right)/RT - RT(\partial \beta_{T0}/\partial P)_T \tag{12}$$

where $K_C = -(\partial V_C/\partial P)_T$ is the compressibility of the cavity enclosing the solute; $<\Delta K_T> = \sum_{j=0}^{n/r} \sum_{i=0}^{n-jr} \alpha_{ij} \Delta K_{Tij}$ is the ensemble average change in compressibility associated with direct solute–solvent interactions; $\Delta K_{Tij} = -(\partial \Delta V_{ij}/\partial P)_T$ is the compressibility effect of the formation of the solvated complex with i water and j cosolvent molecules; and $<\Delta V^2> = \sum_{j=0}^{n/r} \sum_{i=0}^{n-jr} \alpha_{ij} \Delta V_{ij}^2$.

The partial molar expansibility, E°, of a solute is the temperature slope of its partial molar volume, V°:

$$\begin{aligned}E^\circ &= E_C + <\Delta E> + (<\Delta H \Delta V> - <\Delta H><\Delta V>)/RT^2 \\ &\quad + R\left[\beta_{T0} + T(\partial \beta_{T0}/\partial T)_P\right]\end{aligned} \tag{13}$$

where $E_C = (\partial V_C/\partial T)_P$ is the expansibility of the cavity enclosing the solute, $<\Delta E> = \sum_{j=0}^{n/r} \sum_{i=0}^{n-jr} \alpha_{ij} \Delta E_{ij}$ is the ensemble average change in expansibility associated with direct solute–solvent interactions; $\Delta E_{ij} = (\partial \Delta V_{ij}/\partial T)_P$ is the expansibility effect of the formation of the solvated complex with i water and j cosolvent molecules; $<\Delta H> = \sum_{j=0}^{n/r} \sum_{i=0}^{n-jr} \alpha_{ij} \Delta H_{ij}$ is the ensemble average change in enthalpy associated with direct solute–solvent interactions; $\Delta H_{ij} = -RT^2[\partial(\Delta G_{ij}/RT)/\partial T]_P$ is the enthalpy effect of the formation of the solvated complex with i water and j cosolvent molecules; and $<\Delta H \Delta V> = \sum_{j=0}^{n/r} \sum_{i=0}^{n-jr} \alpha_{ij} \Delta H_{ij} \Delta V_{ij}$.

For practical applications, Eqs. (11)–(13) can be simplified under the assumption of n identical and independent binding sites for the principal solvent (water) and, hence, n/r binding sites for cosolvent in each analyzed solute. The elementary solvation reactions involving a cosolvent-binding site can be presented as follows:

$$S_0 + rW \leftrightarrows SW_r \qquad \text{(Reaction 2)}$$

$$S_0 + O \leftrightarrows SO \qquad \text{(Reaction 3)}$$

where S_0 denotes the dry (unsolvated) binding site.

Based on the combinatorial approach, the total concentration of a solute with n/r identical and independent cosolvent-binding sites in water, $[S_1]$, and a concentrated cosolvent solution, $[S_3]$, are given by $[S_1] = [S_{01}](1 + k_1 a_{10}^r)^{n/r}$ and $[S_3] = [S_{03}](1 + k_1 a_1^r + k_3 a_3)^{n/r}$, respectively; where $[S_{01}]$ and $[S_{03}]$ are the concentrations of unsolvated solute in water and cosolvent solution, respectively; a_{10} and a_1 are the activities of water in the absence and presence of cosolvent, respectively; a_3 is the activity of cosolvent; and k_1 and k_3 are the elementary binding constants for Reactions 2 and 3, respectively. Following a chain of simple steps, one can derive an equation for a change in volume accompanying the transfer of a solute from water to a concentrated cosolvent solution [48,50]:

$$\Delta V^\circ = \Delta V_C - \gamma_1 n \Delta V^\circ_1 + \Delta V (n/r)(a_3/a_1^r)k \Big/ \left[1 + (a_3/a_1^r)k\right] \tag{14}$$

where ΔV_C is the differential cavity volume in a concentrated cosolvent solution and water; $k = k_3/k_1$ is the equilibrium constant for the reaction in which a cosolvent molecule replaces r water molecules at the binding site; $\Delta V = \Delta V_0 + \gamma_1 r \Delta V^\circ_1 - \gamma_3 \Delta V^\circ_3$ is the change in volume associated with replacement of water with cosolvent at the binding site in a concentrated cosolvent solution; ΔV_0 is the exchange volume in an ideal solution; ΔV°_1 and ΔV°_3 are the excess partial molar volumes of water and cosolvent in a concentrated solution; and γ_1 and γ_3 are the correction factors reflecting the influence of the bulk solvent on the properties of solvating water and cosolvent, respectively. The values of γ_1 and γ_3 may change from 0 (the properties of the solvation shell change in parallel with those of the bulk) to 1 (the properties of the solvation shell are independent of those of the bulk).

Differentiating Eq. (14) with respect to pressure, one obtains the relationship for a change in compressibility associated with the water-to-cosolvent transfer of a solute:

$$\Delta K_T^\circ = \Delta K_{TC} - \gamma_1 n \Delta K_{T1}^\circ + \Delta K_T (n/r)(a_3/a_1^r)k/[1 + (a_3/a_1^r)k] + \Delta V^2 (n/r)(a_3/a_1^r)k/RT[1 + (a_3/a_1^r)k]^2 \quad (15)$$

where $\Delta K_{TC} = -(\partial \Delta V_C/\partial P)_T$ is the differential compressibility of the cavity enclosing a solute in water and cosolvent solution; $\Delta K_T = \Delta K_{T0} + \gamma_1 r \Delta K_{T1}^\circ - \gamma_3 \Delta K_{T3}^\circ$ is the change in compressibility associated with the replacement of water with cosolvent at the binding site in a concentrated cosolvent solution; ΔK_{T1}° and ΔK_{T3}° are the excess partial molar isothermal compressibilities of water and cosolvent in a concentrated cosolvent solution; $\Delta K_{T0} = -(\partial \Delta V_0/\partial P)_T$ is the change in compressibility associated with the replacement of water with cosolvent at the binding site in an ideal solution.

Differentiating Eq. (14) with respect to temperature yields the relationship for a change in expansibility associated with the water-to-cosolvent transfer of a solute:

$$\Delta E^\circ = \Delta E_C - \gamma_1 n \Delta E^\circ{}_1 + \Delta E (n/r)(a_3/a_1^r)k/[1 + (a_3/a_1^r)k] + (\Delta V \Delta H)(n/r)(a_3/a_1^r)k/RT^2[1 + (a_3/a_1^r)k]^2 \quad (16)$$

where $\Delta E_C = (\partial \Delta V_C/\partial T)_P$ is the differential expansibility of the cavity enclosing a solute in water and cosolvent solution; $\Delta E = \Delta E_0 + \gamma_1 r \Delta E_1^\circ - \gamma_3 \Delta E_3^\circ$ is the change in expansibility associated with the replacement of water with cosolvent at the binding site in a concentrated cosolvent solution; ΔE_1° and ΔE_3° are the excess partial molar expansibilities of water and cosolvent in a concentrated cosolvent solution; $\Delta E_0 = (\partial \Delta V_0/\partial T)_P$ is the change in expansibility associated with the replacement of water with cosolvent at the binding site in an ideal solution.

Eqs. (14)–(16) provide a link between the experimentally measurable observables ΔV°, ΔK_T°, and ΔE° and the equilibrium constant, k, and the intrinsic thermodynamic parameters of the water–cosolvent exchange at the binding sites, ΔV, ΔK_T, ΔE, and ΔH. Consequently, these relationships can be used in practical treatment of urea-dependent volumetric data to evaluate the exchange constant k which quantifies the differential affinity of a solute for cosolvent and water.

3.4. Cavity volume

To analyze experimental volumetric data within the framework of Eqs. (14) to (16), one needs to estimate a change in cavity volume, V_C, which accompanies the transfer of a solute from water to a cosolvent solution. Any significant change in V_C will affect the values of ΔV°, ΔK_T°, and ΔE°. The cavity volume, V_C, in a mixed solvent can be computed based on the concepts of scaled particle theory (SPT) in which the solute and solvent molecules are approximated by a mixture of hard spheres [51]. It should be noted that SPT has been subsequently extended to include solutes of arbitrary shapes [52–54]. However, the "spherical" version of SPT is simpler and has been more extensively used in practical calculations. Within the framework of SPT, the cavity volume can be computed from the equation [51]:

$$V_C = (\beta_{T0}/\alpha_0 T)H_C + N_A \pi d_S^3/6 \quad (17)$$

where β_{T0} and α_0 are, respectively, the coefficients of isothermal compressibility and thermal expansibility of the solvent; N_A is Avogadro's number; d_S is the hard sphere diameter of a solute molecule. The enthalpy of cavity formation, H_C, is given by the relationship [55]:

$$H_C = \left[\alpha_0 RT^2/(1-\xi_3)\right]\left[\xi_3 + 3\xi_2 d_S/(1-\xi_3) + 3\xi_1 d_S^2/(1-\xi_3) + 9\xi_2^2 d_S^2/(1-\xi_3)^2\right] \quad (18)$$

where $\xi_k = (\pi N_A/6)\sum_{i=1}^{m} C_i d_i^k$; k has the values of 1, 2, and 3; m is the number of solvent components; C_i and d_i are, respectively, the molar concentration and the molecular diameter of the *i*-th solvent component.

SPT-based calculations critically depend on the specific choice of the hard sphere diameters d_i in Eqs. (17) and (18) as well as on the precise values of component concentrations C_i [56]. Molecules of biological significance are generally non-spherical. The problem of approximation of a complex molecular shape by a sphere with subsequent determination of effective diameters of nonspherical molecules does not have any universal solution. Different approaches may yield significantly different diameters [56]. Ambiguities exist not only with respect to solutes and water-miscible cosolvents, such as urea or glycine betaine, but also with respect to the size of a water molecule itself. The size of a water molecule depends on the extent of its interactions with its neighbors; the effective diameter of a hydrogen bonded molecule is 2.8 Å, while the diameter of a water molecule engaged only in van der Waals interactions is 3.2 Å [57]. Liquid water contains both hydrogen bonding and purely van der Waals interactions.

With these potential problems and uncertainties kept in mind, Eqs. (17) and (18) can be used to compute changes in the cavity volume of a spherical particle associated with its transfer from pure water to a binary water–cosolvent mixture. Fig. 1 graphically presents the calculated changes in the cavity volume, ΔV_C, for a spherical particle with a diameter ranging from 4 to 10 Å accompanying its transfer from water to the denaturing osmolyte urea (panel a) and the protective osmolyte glycine betaine (panel b) as a function of osmolyte concentration. In these calculations, the hard-sphere diameter of a water molecule is 2.74 Å [58,59], while the diameter of the urea molecule is 4.41 Å. The latter has been evaluated from SPT-based calculations of changes in volume and compressibility accompanying the water-to-urea transfer of alkali halides [55,58]. However, note that several hard-sphere diameters of the urea molecule have been reported in the literature [56]. For glycine betaine, the hard-sphere diameter of 6.08 Å has been calculated as $d_{GB} = (6V_{GB}/\pi)^{1/3}$, where V_{GB} is the van der Waals volume of glycine betaine.

Fig. 1A and B reveals parabolic-like dependences of ΔV_C on cosolvent concentration for all solute diameters investigated. An initial decrease in ΔV_C at low to moderate cosolvent concentrations is followed by an increase at higher concentrations. The initial decrease is more pronounced for urea, while the subsequent increase is more pronounced for glycine betaine. Cosolvent-dependent changes in the cavity volume, V_C, are on the order of 1% or less of the absolute value of V_C. For solutes with a diameter between 4 and 6 Å (which corresponds to the size of amino acids and their derivatives), changes in V_C are small being on the order of ~1 $cm^3\ mol^{-1}$ or less. Therefore, when analyzing such small solutes, urea- and glycine betaine-induced changes in cavity volume, ΔV_C, in Eq. (14) and, by extension, changes in the intrinsic compressibility, ΔK_C, and expansibility, ΔE_C, of the cavity in Eqs. (15) and (16) can be ignored. Hence, experimental cosolvent-induced changes in the partial molar volume, compressibility, and expansibility of small solutes can be assumed to predominantly reflect alterations in direct solute–solvent and solute–cosolvent interactions.

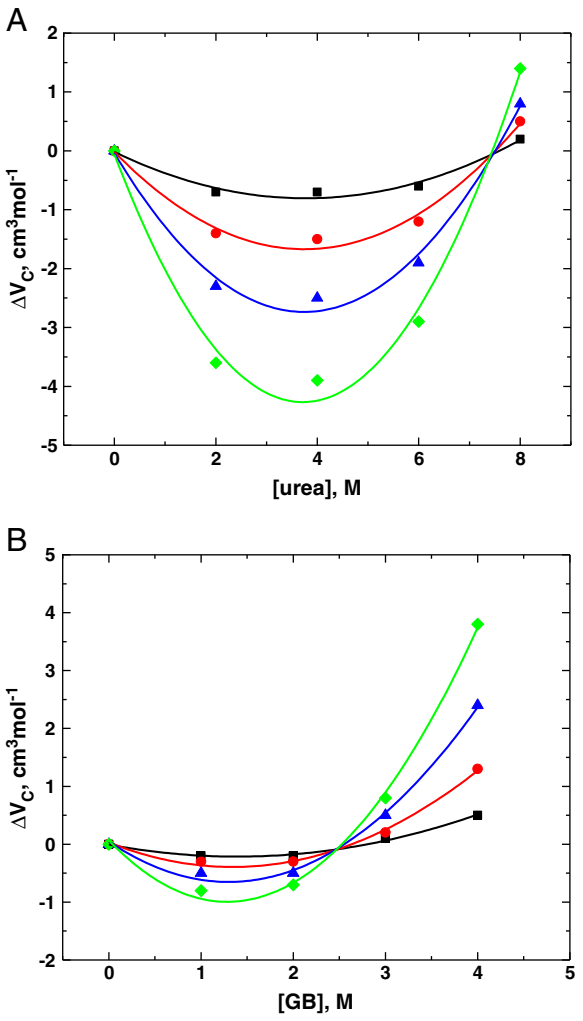

Fig. 1. SPT-based calculated change in the cavity volume, ΔV_C, for a spherical particle with a diameter of 4 (black), 6 (red), 8 (blue), and 10 (green) Å accompanying its transfer from water to urea (panel a) and glycine betaine (panel b) as a function of osmolyte concentration. The concentration of water, [W], as a function of urea concentration, [urea], is given by [W] (M) = 55.34 − 2.45 [urea] − 0.00611 [urea]^2 [48]. The coefficients of isothermal compressibility, β_{T0}, of urea solutions required in Eq. (17) are taken to be equal to 44.8×10^{-6}, 40.2×10^{-6}, 36.8×10^{-6}, 33.9×10^{-6}, and 32.2×10^{-6}bar^{-1} at 0, 2, 4, 6, and 8 M urea, respectively [48]. The concentration of water as a function of glycine betaine concentration, [GB], is given by [W] (M) = 55.34 − 5.46 [GB] + 0.00944 [GB]^2 (Y. L. Shek and T. V. Chalikian, unpublished). The coefficients of isothermal compressibility, β_{T0}, of glycine betaine solutions are taken to be equal to 44.8×10^{-6}, 39.6×10^{-6}, 34.9×10^{-6}, 30.8×10^{-6}, and 27.2×10^{-6}bar^{-1} at 0, 1, 2, 3, and 4 M glycine betaine, respectively (Y. L. Shek and T. V. Chalikian, unpublished).

4. Experimental data

4.1. Low molecular weight molecules

One way to study the effect of cosolvents on the protein stability is based on measuring the thermodynamics of transfer of small molecules mimicking protein groups from water to concentrated osmolyte (cosolvent) solutions [60–63]. In the majority of these studies, the transfer free energies, ΔG_{tr}, of amino acid side chains and the peptide backbone are determined based on the differential solubility measurements and subsequently used to predict the osmolyte-dependent protein stability based on additive calculations [64]. On the other hand, Eqs. (14)–(16) open a way to investigating the transfer energetics based on high precision measurements of the partial molar volume, compressibility, and expansibility of a solute as a function of the cosolvent concentration. Nevertheless, review of the literature reveals scarcity of volumetric data on proteins and/or their small analogs in water–cosolvent mixtures. The partial molar volumes of the 20 naturally occurring zwitterionic amino acids in water and 8 M urea have been reported by Jolicoeur et al. [65]. Comparative analysis reveals that, on average, a zwitterionic amino acid in 8 M urea exhibits a partial molar volume which is 4.2 ± 1.1 cm^3 mol^{-1} higher than that in water. This value is in good agreement with a recent work in which the partial molar volume and adiabatic compressibility of zwitterionic glycine have been measured at 0, 2, 4, 6, and 8 M urea [48]. The differential partial molar volume of glycine in water and 8 M urea is 3.6 ± 0.5 cm^3 mol^{-1} [48].

On a similar note, Poklar et al. have measured an increase in the partial molar volume of a number of zwitterionic dipeptides following their transfer from water to concentrated solutions of urea, methylurea, N,N′-dimethylurea, or ethylurea solutions [66]. This experimental observation has been qualitatively interpreted as resulting from a decrease in electrostriction when water is replaced by urea or alkylurea in the solvation shell of a solute [66].

The most complete and systematic set of urea-dependent volumetric properties of low molecular weight model compounds mimicking proteins has been recently reported by Lee et al. [50]. In this work, high precision density and sound velocity measurements have been employed to determine the partial molar volumes and adiabatic compressibilities of N-acetyl amino acid amides, N-acetyl amino acid methylamides, N-acetyl amino acids, and short oligoglycines as a

Table 1
Partial molar volumes, V° (cm^3 mol^{-1}), of low molecular weight protein analogs as a function of urea concentration at 25 °C.[a]

Compounds	0 M	2 M	4 M	6 M	8 M
N-Ac-Gly-NH_2	90.5 ± 0.1	91.1 ± 0.1	91.3 ± 0.1	91.5 ± 0.1	91.7 ± 0.3
N-Ac-Gly-NH-Me	108.8 ± 0.4	108.7 ± 0.3	108.8 ± 0.1	108.8 ± 0.3	108.8 ± 0.2
N-Ac-Gly	88.3 ± 0.2	88.6 ± 0.1	88.7 ± 0.1	88.8 ± 0.2	89.0 ± 0.2
N-Ac-Ala-NH_2	107.3 ± 0.3	108.1 ± 0.1	108.3 ± 0.1	108.5 ± 0.3	108.6 ± 0.2
N-Ac-Ala	105.4 ± 0.1	105.7 ± 0.1	106.1 ± 0.1	106.2 ± 0.2	106.4 ± 0.4
N-Ac-Val-NH_2	138.2 ± 0.1	139.0 ± 0.1	139.3 ± 0.2	139.5 ± 0.1	139.9 ± 0.2
N-Ac-Leu-NH_2	155.9 ± 0.2	156.5 ± 0.1	156.8 ± 0.1	157.1 ± 0.1	157.5 ± 0.2
N-Ac-Ile-NH_2	153.7 ± 0.3	154.1 ± 0.2	154.3 ± 0.3	154.7 ± 0.3	155.0 ± 0.2
N-Ac-Pro-NH_2	126.1 ± 0.1	126.5 ± 0.3	126.7 ± 0.1	126.8 ± 0.1	127.0 ± 0.1
N-Ac-Phe-NH_2	170.4 ± 0.3	171.1 ± 0.1	171.6 ± 0.3	172.1 ± 0.3	172.4 ± 0.1
N-Ac-Phe	168.2 ± 0.1	169.0 ± 0.1	169.3 ± 0.1	169.7 ± 0.1	169.9 ± 0.3
N-Ac-Trp-NH_2	192.6 ± 0.1	193.2 ± 0.2	193.7 ± 0.2	193.9 ± 0.2	194.2 ± 0.5
N-Ac-Trp	188.8 ± 0.1	191.0 ± 0.8	191.3 ± 0.3	191.7 ± 0.3	192.1 ± 0.3
N-Ac-Met-NH_2	153.3 ± 0.1	154.3 ± 0.1	154.7 ± 0.4	155.1 ± 0.1	155.2 ± 0.2
N-Ac-Cys	117.9 ± 0.5	119.1 ± 0.1	119.6 ± 0.2	119.8 ± 0.2	120.2 ± 0.1
N-Ac-Tyr-NH_2	172.7 ± 0.2	173.8 ± 0.1	174.3 ± 0.1	174.6 ± 0.1	174.8 ± 0.3
N-Ac-Ser	105.3 ± 0.1	106.0 ± 0.1	106.5 ± 0.1	106.7 ± 0.2	106.9 ± 0.3
N-Ac-Thr	121.3 ± 0.1	122.1 ± 0.5	122.7 ± 0.5	123.1 ± 0.2	123.5 ± 0.4
N-Ac-Asn	122.2 ± 0.1	123.4 ± 0.3	124.0 ± 0.2	124.3 ± 0.1	124.7 ± 0.2
N-Ac-Gln-NH_2	141.3 ± 0.1	142.2 ± 0.2	142.6 ± 0.1	143.0 ± 0.7	143.2 ± 0.2
N-Ac-Asp-NH_2 (pH 2.9[b])	121.1 ± 0.1	122.0 ± 0.2	122.5 ± 0.2	122.7 ± 0.1	123.0 ± 0.1
N-Ac-Glu-NH_2 (pH 3.2[b])	137.3 ± 0.7	138.3 ± 0.1	138.7 ± 0.1	139.2 ± 0.1	139.4 ± 0.2
N-Ac-His-NH-Me (pH 8.7[b])	165.8 ± 0.4	166.2 ± 0.1	166.8 ± 0.1	167.0 ± 0.2	167.3 ± 0.5
N-Ac-Lys-NH_2 HCl (pH 4.4[b])	172.5 ± 0.4	174.6 ± 0.5	175.9 ± 0.3	176.8 ± 0.2	177.4 ± 0.1
N-Ac-Arg-NH_2 CH_3COOH (pH 6.3[b])	211.6 ± 0.3	213.1 ± 0.3	214.0 ± 0.2	214.9 ± 0.3	215.5 ± 0.2
Glycine	43.0 ± 0.2	44.1 ± 0.2	45.1 ± 0.3	46.0 ± 0.3	46.6 ± 0.3
Diglycine	76.2 ± 0.3	77.8 ± 0.3	79.3 ± 0.4	80.3 ± 0.4	80.9 ± 0.4
Triglycine	111.9 ± 0.3	113.7 ± 0.3	115.1 ± 0.3	116.5 ± 0.4	117.4 ± 0.5
Tetraglycine	149.8 ± 0.4	151.8 ± 0.5	153.2 ± 0.5	154.4 ± 0.6	155.0 ± 0.7
Pentaglycine	186.1 ± 1.5	187.7 ± 1.6	189.0 ± 1.7	190.2 ± 1.8	190.9 ± 1.9
N-methyl acetamide	73.9 ± 0.1	73.6 ± 0.1	73.2 ± 0.1	73.1 ± 0.2	73.0 ± 0.1

[a] From Supplementary Material to ref. [50].
[b] Experimental pH in pure water.

Table 2
Partial molar adiabatic compressibilities, $K°_S$ (10^{-4} cm^3 mol^{-1} bar^{-1}), of low molecular weight protein analogs as a function of urea concentration at 25 °C.[a]

Compounds	0 M	2 M	4 M	6 M	8 M
N-Ac-Gly-NH_2	−1.7 ± 0.4	4.2 ± 0.5	9.0 ± 0.5	12.1 ± 0.7	15.0 ± 0.5
N-Ac-Gly-NH-Me	1.4 ± 0.4	8.5 ± 0.6	13.2 ± 0.7	16.8 ± 0.7	20.1 ± 0.4
N-Ac-Gly	1.8 ± 0.4	8.7 ± 0.4	13.5 ± 1.0	16.5 ± 1.5	19.3 ± 0.9
N-Ac-Ala-NH_2	−0.6 ± 0.3	6.9 ± 0.7	12.2 ± 1.0	15.7 ± 1.5	19.0 ± 0.2
N-Ac-Ala	4.6 ± 0.5	12.4 ± 0.5	18.5 ± 0.4	21.7 ± 0.3	24.7 ± 0.7
N-Ac-Val-NH_2	−1.1 ± 0.1	10.8 ± 0.3	18.9 ± 0.8	23.9 ± 0.1	28.4 ± 0.5
N-Ac-Leu-NH_2	−1.3 ± 0.4	12.9 ± 0.2	22.9 ± 0.3	28.7 ± 1.5	33.4 ± 0.4
N-Ac-Ile-NH_2	−2.6 ± 0.1	10.1 ± 0.4	19.8 ± 0.7	27.7 ± 0.6	33.5 ± 0.4
N-Ac-Pro-NH_2	−5.7 ± 0.4	5.4 ± 1.0	11.8 ± 0.6	16.6 ± 1.0	19.9 ± 0.9
N-Ac-Phe-NH_2	−0.6 ± 0.3	13.3 ± 0.2	22.2 ± 0.5	28.3 ± 0.9	33.3 ± 0.2
N-Ac-Phe	5.4 ± 0.4	18.7 ± 1.0	27.4 ± 0.2	33.3 ± 0.3	37.9 ± 0.6
N-Ac-Trp-NH_2	2.3 ± 0.5	15.2 ± 1.0	23.3 ± 0.6	29.1 ± 0.2	34.1 ± 1.4
N-Ac-Trp	5.4 ± 0.5	19.7 ± 1.0	29.0 ± 0.4	36.3 ± 1.3	41.0 ± 0.5
N-Ac-Met-NH_2	−3.1 ± 0.2	10.9 ± 0.6	19.3 ± 0.4	23.5 ± 0.3	27.2 ± 0.5
N-Ac-Cys	−3.1 ± 0.4	8.5 ± 0.5	15.2 ± 0.7	18.9 ± 0.2	22.5 ± 0.6
N-Ac-Tyr-NH_2	6.1 ± 0.3	17.2 ± 0.4	24.2 ± 0.6	28.6 ± 0.8	31.4 ± 0.4
N-Ac-Ser	−0.5 ± 0.4	6.7 ± 0.1	11.6 ± 1.2	14.6 ± 0.3	17.5 ± 0.3
N-Ac-Thr	−0.4 ± 0.5	9.6 ± 0.7	16.1 ± 1.2	20.7 ± 1.2	23.6 ± 0.6
N-Ac-Asn	−1.5 ± 0.4	7.5 ± 0.8	13.6 ± 0.4	17.3 ± 0.8	20.1 ± 0.4
N-Ac-Gln-NH_2	−2.7 ± 0.1	6.0 ± 0.3	11.9 ± 0.4	16.0 ± 0.8	19.2 ± 0.9
N-Ac-Asp-NH_2 (pH 2.9[b])	−3.7 ± 0.2	4.3 ± 0.2	10.1 ± 0.6	13.4 ± 0.5	16.5 ± 0.8
N-Ac-Glu-NH_2 (pH 3.2[b])	−1.4 ± 0.7	7.9 ± 1.0	14.3 ± 0.6	19.1 ± 0.1	22.7 ± 0.5
N-Ac-His-NH-Me (pH 8.7[b])	3.2 ± 0.6	13.4 ± 1.0	20.9 ± 0.4	24.9 ± 0.3	28.8 ± 0.5
N-Ac-Lys-NH_2HCl (pH 4.4[b])	−25.8 ± 0.4	−8.2 ± 0.5	4.1 ± 0.9	12.1 ± 0.4	18.6 ± 0.3
N-Ac-Arg-NH_2CH_3COOH (pH 6.3[b])	−27.0 ± 0.4	−7.0 ± 0.5	5.9 ± 1.0	15.4 ± 0.9	21.3 ± 0.6
Glycine	−26.8 ± 0.2	−20.2 ± 0.3	−14.8 ± 0.5	−10.9 ± 0.5	−8.1 ± 0.5
Diglycine	−40.3 ± 0.4	−29.9 ± 0.4	−21.8 ± 0.4	−16.4 ± 0.5	−12.6 ± 0.5
Triglycine	−44.7 ± 0.4	−31.6 ± 0.5	−22.3 ± 0.5	−15.1 ± 0.6	−9.8 ± 0.6
Tetraglycine	−45.2 ± 0.5	−31.3 ± 0.6	−20.8 ± 0.6	−12.8 ± 0.8	−7.4 ± 0.9
Pentaglycine	−48.2 ± 1.4	−31.8 ± 1.5	−20.1 ± 1.3	−11.4 ± 1.3	−5.2 ± 1.5
N-methyl acetamide	8.9 ± 0.4	11.6 ± 0.3	14.2 ± 0.4	17.2 ± 0.5	19.8 ± 0.3

[a] From Supplementary Material to ref. [50].
[b] Experimental pH in pure water.

function of urea concentration. The individual compounds have been selected so as to collectively cover the glycyl unit (–CH_2CONH–) and the 19 naturally occurring amino acid side chains. Tables 1 and 2 present the partial molar volumes, V°, and adiabatic compressibilities, $K°_S$, of the solutes studied at 0, 2, 4, 6, and 8 M urea [50]. Note that the urea-induced changes in volume (see Table 1) are much less pronounced relative to the changes in compressibility (see Table 2). This observation is not unexpected given the fact that the intrinsic (geometric) volume of a solute is the main component of its partial molar volume, while the solvation component is relatively modest. In contrast, the partial molar adiabatic compressibility, $K°_S$, of a small molecule is overwhelmingly determined by its solvation properties (solute–solvent interactions) with the intrinsic contribution being negligibly small [36–38,67]. In general, volume is a rather conservative property with characteristically small changes associated with virtually all biochemical and biophysical processes including conformational transitions and binding reactions of macromolecules [37,38,67–70].

The measured urea-dependent volumetric parameters have been used to evaluate the volumetric contributions of the glycyl unit and all naturally occurring amino acid side chains [50]. The volume or compressibility contributions of the 19 amino acid side chains have been calculated as the difference in the partial molar volume, V°, or adiabatic compressibility, $K°_S$, between the amino acid and its respective glycine derivatives [50]. These volumetric contributions have been further analyzed within the framework of Eqs. (14) and (15) to determine the exchange constants, k, and the elementary changes in volume, ΔV_0, and adiabatic compressibility, ΔK_{S0} [50]. Note that the exchange constants, k, are directly related to the change in free energy of direct solute–solvent interactions associated with the transfer of a solute from pure water to a concentrated water–urea mixture [50]:

$$\Delta\Delta G_I = -(n/r)RT\,ln\left[(a_1/a_{10})^r + k(a_3/a_{10}^r)\right] \quad (19)$$

where a_{10} is the activity of water in the absence of urea.

The exchange constants, k, determined for the amino acid side chains and the glycyl unit correspond to changes in the interaction free energies ranging from highly favorable to slightly unfavorable [50]. More quantitatively, with the exception of serine and aspartic acid, the transfer of all the amino acid side chains and the glycyl unit from water to 2 M urea is accompanied by favorable changes in interaction free energy [50]. These results support the direct mechanism of urea action. More specifically, they are consistent with the picture in which urea denatures a protein by concerted action *via* favorable solute–cosolvent interactions with a wide range of protein groups, including the peptide backbone and most amino acid side chains [50].

The volume, ΔV_0, and compressibility, ΔK_{S0}, changes accompanying an elementary reaction in which a urea molecule replaces water molecules in the solvation shell of a solute represent quantitative thermodynamic measures of the change in solvation associated with the transfer of the solute from water to a water–urea mixture. The values of ΔV_0 and ΔK_{S0} are influenced by a number of factors including the release of water molecules from the contact areas of the solute and urea molecules, solute–urea interactions, and the differential thermal volumes of the solute and urea molecules in their bound relative to the unbound (free in solution) states [71].

4.2. Proteins

A few studies have reported changes in volume and adiabatic compressibility accompanying the urea- and guanidinium chloride-induced denaturation transitions of chymotrypsinogen A, ribonuclease A, and lysozyme [72–77]. Table 3 lists results of these studies. Inspection of the tabulated data reveals that, despite the significant numerical differences between the reported values of Δv and Δk_S for lysozyme, the transitions are characterized by negative changes in volume and compressibility. Interpretation of these volumetric results

Table 3
Changes in volume, Δv, and adiabatic compressibility, Δk_S, accompanying urea- and GuHCl-induced protein denaturation at 25 °C.

Protein	Δv, $cm^3\ g^{-1}$	Δk_S, $10^{-6} cm^3\ g^{-1}\ bar^{-1}$
Chymotrypsinogen A[a] (urea, pH 7.0)	−0.014	
Ribonuclease A[b] (GuHCl, pH 2.0)	−0.061 ± 0.045	−18 ± 4
Lysozyme[c] (GuHCl, pH 5.2)	−0.0038	
Lysozyme[d] (GuHCl, pH 1.5)	−0.0091	−1.8
Lysozyme[e] (GuHCl, pH 4.0)	−0.084	−11
Lysozyme[f] (GuHCl, water)	0 ± 0.01	−3.0

[a] Ref. [72].
[b] Ref. [74].
[c] Ref. [73].
[d] Ref. [77].
[e] Ref. [75].
[f] Ref. [76].

has been performed by invoking changes in intrinsic packing and hydration, as well as interactions of cosolvent with the protein in its native and unfolded conformations.

The precision of cosolvent-dependent volumetric measurements and the veracity of ensuing interpretations depend on the reliability of determination of the pre- and post-denaturational baselines. Determination of post-denaturational baselines is especially problematic due to the experimental challenges related to measurements at extremely high denaturant concentrations. Additive calculations based on the group contributions for the amino acid side chains and the glycyl unit can be used to evaluate the volumetric properties of fully extended polypeptide chains as the extreme case of the unfolded conformation. These calculations should be based on the amino acid sequence of the polypeptide using the following additive scheme:

$$x^\circ = \Big[X^\circ(\text{trigly}) + \Delta X_{NH_2}/\left(1+10^{pH-pK_{aNH_2}}\right) - \Delta X_{COOH}/\left(1+10^{pK_{aCOOH}-pH}\right) + (n-3)X(-CH_2CONH-) + \sum_{i=1}^{n} X_i(-R) + \sum_{j=1}^{l} \Delta X_j/\left(1+10^{pH-pK_{aj}}\right) - \sum_{k=1}^{m} \Delta X_k/\left(1+10^{pK_{ak}-pH}\right)\Big]/M \quad (20)$$

where x° is the partial specific volume or adiabatic compressibility of the protein in question; X°(trigly) is the partial molar volume or adiabatic compressibility of triglycine; ΔX_{NH2} and ΔX_{COOH} are the protonation volumes and compressibilities of the amino and carboxyl termini, respectively; pK_{aNH2} and pK_{aCOOH} are the dissociation constants of the amino and carboxyl termini, respectively; $X_i(-R)$ is the volume or compressibility contribution of the *i*-th amino acid side chain [for an ionizable side chain, $X_i(-R)$ corresponds to the neutral state]; *n* is the number of amino acid residues in the polypeptide chain; *l* is the number of basic side chains; pK_{aj} and ΔX_j are the dissociation constant and the protonation volume or compressibility of the *j*-th basic side chains; *m* is the number of acidic side chains; pK_{ak} and ΔX_k are the dissociation constant and the protonation volume or compressibility of the *k*-th acidic side chain; and M is the molecular weight of the protein.

Fig. 2 plots the additively calculated partial specific adiabatic compressibilities of the fully extended conformations of ribonuclease A, lysozyme, ubiquitin, apocytochrome c, apomyoglobin, and α-chymotrypsinogen A at pH 7 as a function of urea. The calculations were carried out with Eq. (20) in conjunction with the urea-dependent compressibility data on triglycine, the compressibility group contributions of the side chains and the glycyl unit, and the pH-dependent volumetric data on ionization of titrable amino acid side chains from Supplementary Material to ref. [50]. The plots in Fig. 2 exhibit a great deal of similarity with the differences being on the order of $\pm 1\times10^{-6}\ cm^3\ g^{-1}\ bar^{-1}$. In contrast, the values of k°_S of the same proteins in the native conformation are significantly different ranging from 0 to $8\times10^{-6}\ cm^3\ g^{-1}\ bar^{-1}$ [78]. Fig. 3 presents simulated

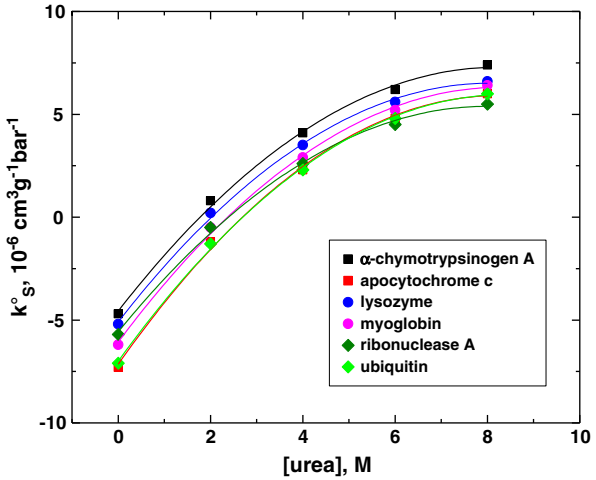

Fig. 2. Partial specific adiabatic compressibilities of the fully extended conformations of ribonuclease A, lysozyme, ubiquitin, apocytochrome c, apomyoglobin, and α-chymotrypsinogen A at pH 7 additively calculated as a function of urea with Eq. (20).

changes in the partial specific adiabatic compressibilities, k°_S, of three hypothetical globular proteins induced by urea-induced denaturation. The simulations are based on the linear extrapolation model of protein denaturation [79,80]. In the simulations, the urea dependence of the partial specific adiabatic compressibility, k°_S, of the unfolded conformation was modeled by the average urea dependence calculated for the six unfolded proteins shown in Fig. 2. The rate of the urea-dependent change in the partial specific adiabatic compressibility, k°_S, of the native conformation is modeled by one third of that of the fully extended conformation given the ratio of the solvent accessible surface areas of the two conformations [81].

As is seen from Fig. 3, the protein with the highest initial partial specific adiabatic compressibility, k°_S, of $5\times10^{-6}\ cm^3\ g^{-1}\ bar^{-1}$ exhibits a decrease in compressibility caused by the urea-induced denaturation (with a midpoint of 4 M). By contrast, the protein with the lowest initial k°_S ($0\ cm^3\ g^{-1}\ bar^{-1}$) exhibits a positive change in compressibility accompanying the denaturation. The protein with the intermediate initial value of k°_S of $1.5\times10^{-6}\ cm^3\ g^{-1}\ bar^{-1}$ exhibits an insignificant change in compressibility upon the transition. It appears, therefore, that the magnitude and even the sign of a change in compressibility accompanying the urea-induced unfolding of a

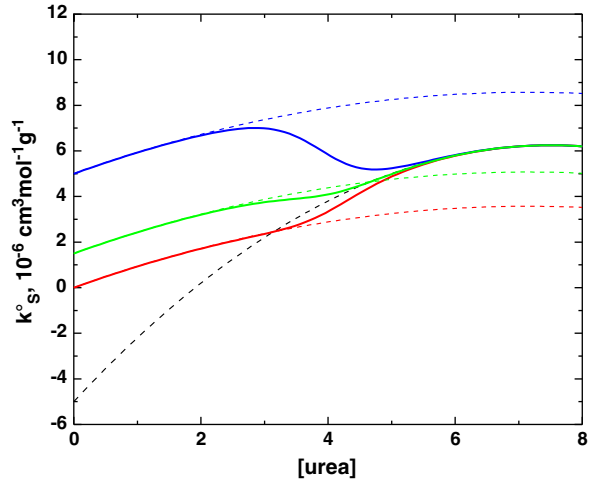

Fig. 3. Urea-dependences of the partial specific adiabatic compressibilities, k°_S, of hypothetical globular proteins simulated based on the linear extrapolation model of protein denaturation [79,80]; $x = x_N + (x_D - x_N)/[1+\exp(-(\Delta G_0 - m[\text{urea}])/RT)]$, with $\Delta G_0 = 6$ kcal/mol and $m = 1.5$ kcal/mol/M.

protein are mainly determined by its initial partial specific adiabatic compressibility. This result contrasts the compressibility behavior of globular proteins in water. In water, a change in protein compressibility caused by a conformational transition depends on the type of the transition more than on the protein [38,82,83]. Native-to-unfolded transitions are all characterized by large negative changes in compressibility [38,82,83]. Urea-induced denatured protein states represent the most unfolded and solvent exposed conformation among protein conformations. Nevertheless, the plots presented in Fig. 3 suggest that the urea-induced protein unfolding may be accompanied by positive or negative changes in compressibility.

The partial compressibility of a protein can be effectively presented as the sum of the intrinsic, k_M, and solvation, Δk_{solv}, contributions [33,34,36,38,67,83]:

$$k^\circ_S = k_M + \Delta k_{solv}. \quad (21)$$

The intrinsic compressibility, k_M, reflects the presence of compressible voids inside the water-inaccessible core(s) of the protein. The solvation contribution, Δk_{solv}, is negative in water, however becomes increasingly positive at elevated urea concentration increases due to the replacement of water of hydration by urea molecules [50]. Protein unfolding which is accompanied by disruption of the compressible interior and solvent-exposure of previously buried atomic groups with concomitant increase in solvation causes a decrease in k_M and an increase in the absolute value of Δk_{solv}. In water, where Δk_{solv} is negative, changes in k_M and Δk_{solv} are both negative which leads to the overall negative sign of the change in k°_S. In concentrated urea solutions, where Δk_{solv} is positive, the denaturation-induced enhancement of protein solvation will render a change in Δk_{solv} positive which may or may not offset the decrease in k_M. Thus, a change in compressibility accompanying the urea-induced unfolding of a protein may be either positive or negative depending on the relative changes in Δk_{solv} and k_M.

Further experimental studies are needed to test the veracity of the simulations presented in Figs. 2 and 3 and the ensuing conclusions. Such investigations are currently under way in our laboratory. It should be noted that the comparison of experimental data on the compressibility of urea-induced denatured states with the results of additive calculations may be potentially used to estimate the extent of protein unfolding. For example, the steeper urea-dependence of k°_S of the fully extended conformation coupled with more positive values of k°_S at high urea concentrations relative to the real protein would be consistent with a picture in which the protein retains water inaccessible residues. However, should these water-inaccessible residues form a sizeable and compressible cluster(s), the partial compressibility of the real protein may exceed that calculated for the fully extended conformation.

5. Concluding remarks

With recent experimental and theoretical advances, properly designed volumetric measurements have proven useful for characterization of the differential thermodynamic properties of solute–water and solute–cosolvent interactions in a binary solvent. Among these properties, are the equilibrium constant for a reaction in which a cosolvent molecule binds to a solute replacing waters of hydration as well as changes in volume, compressibility, and expansibility associated with such a reaction. The latter represent the volumetric signature of solvation in binary solvents.

Volumetric measurements in the solutions of low-molecular weight model compounds in water–urea mixtures have begun to provide us with novel insights into the differential interactions of various protein groups with water and urea. These studies, while still in their embryonic state, show promising tendencies for subsequent extension to solvent-induced stabilization/destabilization of the native conformation of the protein as well as characterization of the nature of solvent-induced denatured states. Such extensions require a further build-up of systematic volumetric libraries on proteins and their simple analogs in binary mixtures of water with denaturing and protecting osmolytes. Experimental studies should be augmented by parallel theoretical investigations focusing on both the simulation of the volumetric properties of proteins and protein analogs in water–cosolvent mixtures and further development of theoretical frameworks for molecular interpretation of experimental volumetric results.

Acknowledgement

This work was supported by a grant from the Natural Sciences and Engineering Research Council of Canada to TVC.

References

[1] S.N. Timasheff, Water as ligand: preferential binding and exclusion of denaturants in protein unfolding, Biochemistry 31 (1992) 9857–9864.
[2] S.N. Timasheff, Protein hydration, thermodynamic binding, and preferential hydration, Biochemistry 41 (2002) 13473–13482.
[3] Y. Levy, J.N. Onuchic, Water mediation in protein folding and molecular recognition, Annu. Rev. Biophys. Biomol. Struct. 35 (2006) 389–415.
[4] P.H. Yancey, M.E. Clark, S.C. Hand, R.D. Bowlus, G.N. Somero, Living with water stress: evolution of osmolyte systems, Science 217 (1982) 1214–1222.
[5] J.A. Schellman, Protein stability in mixed solvents: a balance of contact interaction and excluded volume, Biophys. J. 85 (2003) 108–125.
[6] P.H. Yancey, Organic osmolytes as compatible, metabolic and counteracting cytoprotectants in high osmolarity and other stresses, J. Exp. Biol. 208 (2005) 2819–2830.
[7] S.N. Timasheff, The control of protein stability and association by weak interactions with water: how do solvents affect these processes? Annu. Rev. Biophys. Biomol. Struct. 22 (1993) 67–97.
[8] J. Rosgen, B.M. Pettitt, D.W. Bolen, An analysis of the molecular origin of osmolyte-dependent protein stability, Protein Sci. 16 (2007) 733–743.
[9] S. Shimizu, Estimating hydration changes upon biomolecular reactions from osmotic stress, high pressure, and preferential hydration experiments, Proc. Natl Acad. Sci. USA 101 (2004) 1195–1199.
[10] S. Shimizu, N. Matubayasi, Preferential hydration of proteins: a Kirkwood–Buff approach, Chem. Phys. Lett. 420 (2006) 518–522.
[11] S.N. Timasheff, Control of protein stability and reactions by weakly interacting cosolvents: the simplicity of the complicated, Adv. Protein Chem. 51 (1998) 355–432.
[12] M.T. Record Jr., C.F. Anderson, Interpretation of preferential interaction coefficients of nonelectrolytes and of electrolyte ions in terms of a two-domain model, Biophys. J. 68 (1995) 786–794.
[13] J. Rosgen, Molecular basis of osmolyte effects on protein and metabolites, Meth. Enzymol. 428 (2007) 459–486.
[14] P.E. Smith, Cosolvent interactions with biomolecules: relating computer simulation data to experimental thermodynamic data, J. Phys. Chem. B 108 (2004) 18716–18724.
[15] P.E. Smith, Local chemical potential equalization model for cosolvent effects on biomolecular equilibria, J. Phys. Chem. B 108 (2004) 16271–16278.
[16] P.E. Smith, Chemical potential derivatives and preferential interaction parameters in biological systems from Kirkwood–Buff theory, Biophys. J. 91 (2006) 849–856.
[17] S. Shimizu, C.L. Boon, The Kirkwood–Buff theory and the effect of cosolvents on biochemical reactions, J. Chem. Phys. 121 (2004) 9147–9155.
[18] S. Shimizu, D.J. Smith, Preferential hydration and the exclusion of cosolvents from protein surfaces, J. Chem. Phys. 121 (2004) 1148–1154.
[19] S. Shimizu, Estimation of excess solvation numbers of water and cosolvents from preferential interaction and volumetric experiments, J. Chem. Phys. 120 (2004) 4989–4990.
[20] I.L. Shulgin, E. Ruckenstein, A protein molecule in an aqueous mixed solvent: fluctuation theory outlook, J. Chem. Phys. 123 (2005) 054909.
[21] J.M. Schurr, D.P. Rangel, S.R. Aragon, A contribution to the theory of preferential interaction coefficients, Biophys. J. 89 (2005) 2258–2276.
[22] V. Pierce, M. Kang, M. Aburi, S. Weerasinghe, P.E. Smith, Recent applications of Kirkwood–Buff theory to biological systems, Cell Biochem. Biophys. 50 (2008) 1–22.
[23] M.B. Gee, P.E. Smith, Kirkwood–Buff theory of molecular and protein association, aggregation, and cellular crowding, J. Chem. Phys. 131 (2009) 165101.
[24] D.G. Hall, Kirkwood–Buff theory of solutions. An alternative derivation of part of it and some applications, Trans. Faraday Soc. 67 (1971) 2516–2524.
[25] A. Ben-Naim, Solute and solvent effects on chemical equilibria, J. Chem. Phys. 63 (1975) 2064–2073.
[26] A. Ben-Naim, Statistical Thermodynamics for Chemists and Biochemists, Plenum Press, New York, London, 2002.
[27] A. Ben-Naim, Molecular Theory of Solutions, Oxford University Press, Oxford, 2006.

[28] A. Ben-Naim, Inversion of Kirkwood–Buff theory of solutions: application to water–ethanol system, J. Chem. Phys. 67 (1977) 4884–4890.
[29] J.A. Schellman, Destabilization and stabilization of proteins, Q. Rev. Biophys. 38 (2005) 351–361.
[30] P.R. Davis-Searles, A.J. Saunders, D.A. Erie, D.J. Winzor, G.J. Pielak, Interpreting the effects of small uncharged solutes on protein-folding equilibria, Annu. Rev. Biophys. Biomol. Struct. 30 (2001) 271–306.
[31] F.J. Millero, A.L. Surdo, C. Shin, Apparent molal volumes and adiabatic compressibilities of aqueous amino acids at 25 °C, J. Phys. Chem. 82 (1978) 784–792.
[32] A.A. Zamyatnin, Amino acid, peptide, and protein volume in solution, Annu. Rev. Biophys. Bioeng. 13 (1984) 145–165.
[33] K. Gekko, H. Noguchi, Compressibility of globular proteins in water at 25 °C, J. Phys. Chem. 83 (1979) 2706–2714.
[34] K. Gekko, Y. Hasegawa, Compressibility–structure relationship of globular proteins, Biochemistry 25 (1986) 6563–6571.
[35] A.P. Sarvazyan, Ultrasonic velocimetry of biological compounds, Annu. Rev. Biophys. Biophys. Chem. 20 (1991) 321–342.
[36] T.V. Chalikian, A.P. Sarvazyan, K.J. Breslauer, Hydration and partial compressibility of biological compounds, Biophys. Chem. 51 (1994) 89–107.
[37] T.V. Chalikian, K.J. Breslauer, Volumetric properties of nucleic acids, Biopolymers 48 (1998) 264–280.
[38] T.V. Chalikian, Volumetric properties of proteins, Annu. Rev. Biophys. Biomol. Struct. 32 (2003) 207–235.
[39] L.N. Lin, J.F. Brandts, J.M. Brandts, V. Plotnikov, Determination of the volumetric properties of proteins and other solutes using pressure perturbation calorimetry, Anal. Biochem. 302 (2002) 144–160.
[40] L. Mitra, N. Smolin, R. Ravindra, C. Royer, R. Winter, Pressure perturbation calorimetric studies of the solvation properties and the thermal unfolding of proteins in solution—experiments and theoretical interpretation, Phys. Chem. Chem. Phys. 8 (2006) 1249–1265.
[41] R. Ravindra, C. Royer, R. Winter, Pressure perturbation calorimetic studies of the solvation properties and the thermal unfolding of staphylococcal nuclease, Phys. Chem. Chem. Phys. 6 (2004) 1952–1961.
[42] J.D. Batchelor, A. Olteanu, A. Tripathy, G.J. Pielak, Impact of protein denaturants and stabilizers on water structure, J. Am. Chem. Soc. 126 (2004) 1958–1961.
[43] H. Inoue, S.N. Timasheff, Preferential and absolute interactions of solvent components with proteins in mixed solvent systems, Biopolymers 11 (1972) 737–743.
[44] S.N. Timasheff, Protein–solvent preferential interactions, protein hydration, and the modulation of biochemical reactions by solvent components, Proc. Natl Acad. Sci. USA 99 (2002) 9721–9726.
[45] C. Tanford, Extension of the theory of linked functions to incorporate the effects of protein hydration, J. Mol. Biol. 39 (1969) 539–544.
[46] R. Chitra, P.E. Smith, Preferential interactions of cosolvents with hydrophobic solutes, J. Phys. Chem. B 105 (2001) 11513–11522.
[47] T.V. Chalikian, On the molecular origins of volumetric data, J. Phys. Chem. B 112 (2008) 911–917.
[48] S.Y. Lee, T.V. Chalikian, Volumetric properties of solvation in binary solvents, J. Phys. Chem. B 113 (2009) 2443–2450.
[49] A. Ben-Naim, Standard thermodynamics of transfer. Uses and misuses, J. Phys. Chem. 82 (1978) 792–803.
[50] S. Lee, Y.L. Shek, T.V. Chalikian, Urea interactions with protein groups: a volumetric study, Biopolymers 93 (2010) 866–879.
[51] R.A. Pierotti, Scaled particle theory of aqueous and non-aqueous solutions, Chem. Rev. 76 (1976) 717–726.
[52] M. Irisa, K. Nagayama, F. Hirata, Extended scaled particle theory for dilute-solutions of arbitrary shaped solutes. An application to solvation free energies of hydrocarbons, Chem. Phys. Lett. 207 (1993) 430–435.
[53] M. Irisa, T. Takahashi, K. Nagayama, F. Hirata, Solvation free energies of nonpolar and polar solutes reproduced by a combination of extended scaled particle theory and the Poisson–Boltzmann equation, Mol. Phys. 85 (1995) 1227–1238.
[54] G. Graziano, Dimerization thermodynamics of large hydrophobic plates: a scaled particle theory study, J. Phys. Chem. B 113 (2009) 11232–11239.
[55] N. Desrosiers, J.E. Desnoyers, Enthalpies, heat capacities, and volumes of transfer of the tetrabutylammonium ion from water to aqueous mixed solvents from the point of view of the scaled particle theory, Can. J. Chem. 54 (1976) 3800–3808.
[56] K.E.S. Tang, V.A. Bloomfield, Excluded volume in solvation: sensitivity of scaled-particle theory to solvent size and density, Biophys. J. 79 (2000) 2222–2234.
[57] G. Graziano, Cavity contact correlation function of water from scaled particle theory, Chem. Phys. Lett. 432 (2006) 84–87.
[58] N. Desrosiers, M. Lucas, Relation between molal volumes and molal compressibilities from the viewpoint of the scaled-particle theory. Prediction of the apparent molal compressibilities of transfer, J. Phys. Chem. 78 (1974) 2367–2369.
[59] O. Likhodi, T.V. Chalikian, Partial molar volumes and adiabatic compressibilities of a series of aliphatic amino acids and oligoglycines in D_2O, J. Am. Chem. Soc. 121 (1999) 1156–1163.
[60] A.J. Wang, D.W. Bolen, A naturally occurring protective system in urea-rich cells: mechanism of osmolyte protection of proteins against urea denaturation, Biochemistry 36 (1997) 9101–9108.
[61] M. Auton, D.W. Bolen, Additive transfer free energies of the peptide backbone unit that are independent of the model compound and the choice of concentration scale, Biochemistry 43 (2004) 1329–1342.
[62] M. Auton, D.W. Bolen, Predicting the energetics of osmolyte-induced protein folding/unfolding, Proc. Natl Acad. Sci. USA 102 (2005) 15065–15068.
[63] M. Auton, L.M. Holthauzen, D.W. Bolen, Anatomy of energetic changes accompanying urea-induced protein denaturation, Proc. Natl Acad. Sci. USA 104 (2007) 15317–15322.
[64] M. Auton, D.W. Bolen, Application of the transfer model to understand how naturally occurring osmolytes affect protein stability, Meth. Enzymol. 428 (2007) 397–418.
[65] C. Jolicoeur, B. Riedl, D. Desrochers, L.L. Lemelin, R. Zamojska, O. Enea, Solvation of amino acid residues in water and urea–water mixtures: volumes and heat capacities of 20 amino acids in water and in 8 molar urea at 25 °C, J. Solution Chem. 15 (1986) 109–128.
[66] N. Poklar, M.M. Senegacnik, F. Sveglj, S. Lapanje, Apparent specific volumes of some dipeptides containing L-Valine and L-Leucine in aqueous alkylurea solutions, Int. J. Pep. Prot. Res. 39 (1992) 415–418.
[67] T.V. Chalikian, K.J. Breslauer, Thermodynamic analysis of biomolecules: a volumetric approach, Curr. Opin. Struct. Biol. 8 (1998) 657–664.
[68] T.V. Chalikian, R. Filfil, How large are the volume changes accompanying protein transitions and binding? Biophys. Chem. 104 (2003) 489–499.
[69] T.V. Chalikian, K.J. Breslauer, On volume changes accompanying conformational transitions of biopolymers, Biopolymers 39 (1996) 619–626.
[70] T.V. Chalikian, R.B. Macgregor Jr., Nucleic acid hydration: a volumetric perspective, Phys. Life Rev. 4 (2007) 91–115.
[71] D.P. Kharakoz, Partial molar volumes of molecules of arbitrary shape and the effect of hydrogen bonding with water, J. Solution Chem. 21 (1992) 569–595.
[72] J. Skerjanc, V. Dolecek, S. Lapanje, Partial specific volume of chymotrypsinogen A in aqueous urea solutions, Eur. J. Biochem. 17 (1970) 160–164.
[73] J. Skerjanc, S. Lapanje, A dilatometric study of the denaturation of lysozyme by guanidine hydrochloride and hydrochloric acid, Eur. J. Biochem. 25 (1972) 49–53.
[74] Y. Tamura, K. Gekko, Compactness of thermally and chemically denatured ribonuclease A as revealed by volume and compressibility, Biochemistry 34 (1995) 1878–1884.
[75] T. Kamiyama, K. Gekko, Compressibility and volume changes of lysozyme due to guanidine hydrochloride denaturation, Chem. Lett. (1997) 1063–1064.
[76] K. Sasahara, N. Sakurai, K. Nitta, The volume and compressibility changes of lysozyme associated with guanidinium chloride and pressure-assisted unfolding, J. Mol. Biol. 291 (1999) 693–701.
[77] T. Hayashi, M. Sakurai, K. Nitta, The volume and compressibility changes associated with protein denaturation, Chem. Lett. (1996) 723–724.
[78] T.V. Chalikian, M. Totrov, R. Abagyan, K.J. Breslauer, The hydration of globular proteins as derived from volume and compressibility measurements: cross correlating thermodynamic and structural data, J. Mol. Biol. 260 (1996) 588–603.
[79] C.N. Pace, K.L. Shaw, Linear extrapolation method of analyzing solvent denaturation curves, Proteins Struct. Func. Genet. Suppl. 4 (2000) 1–7.
[80] J.M. Scholtz, G.R. Grimsley, C.N. Pace, Solvent denaturation of proteins and interpretations of the m value, Meth. Enzymol. 466 (2009) 549–565.
[81] F.M. Richards, Areas, volumes, packing, and protein structure, Annu. Rev. Biophys. Bioeng. 6 (1977) 151–176.
[82] T.V. Chalikian, K.J. Breslauer, Compressibility as a means to detect and characterize globular protein states, Proc. Natl Acad. Sci. USA 93 (1996) 1012–1014.
[83] N. Taulier, T.V. Chalikian, Compressibility of protein transitions, Biochim. Biophys. Acta 1595 (2002) 48–70.